TWELFTH EUROPEAN ROTORCRAFT FORUM

Paper No. 60

AN IMPROVED ASSUMED MODE METHOD FOR ESTIMATING THE MOTION OF A NONUNIFORM ROTOR BLADE

H. Azzam and P. Taylor

Department of Aeronautics and Astronautics
University of Southampton, Southampton, U.K.

September 22 - 25, 1986

Garmisch-Partenkirchen
Federal Republic of Germany

Deutsche Gesellschaft für Luft- und Raumfahrt e. V. (DGLR)
Godesberger Allee 70, D-5300 Bonn 2, F.R.G.

AN IMPROVED ASSUMED MODE METHOD FOR ESTIMATING THE MOTION OF A NONUNIFORM ROTOR BLADE

H. Azzam, Research Fellow, Southampton University
P. Taylor*, Southampton University, U.K.

Abstract

The uncoupled flapwise and torsional motion of a rotating blade is considered in order to demonstrate that the Galerkin method is also applicable to the case of a nonuniform blade whose structural properties vary sharply along its length. Then, a finite element- like- technique of the assumed modes is presented to provide a consistent relation between the deflection and the moment of the nonuniform blade. The concept of the equivalent flapping hinge offset for hingeless blades is reassessed in an attempt to make the flapping equation more representative. Finally, an equivalent elastic twist is proposed in order to partially compensate for the absence of the torsional analysis in the simple rotor programs

Notation

$A_{\ell i}$	:	An element of the inertia matrix
$B_{\ell i}$	:	An element of the stiffness matrix
C	:	Eigenvector
EI	:	Flexural rigidity, Newtons-metre^2
e	:	Equivalent flapping hinge offset, nondimensionalized w.r.t.R.
GJ	:	Torsional rigidity, Newtons-metre^2
G_i	:	Flapwise approximating functions
g_i	:	Flapwise mode shapes, metres or nondimensionalized w.r.t.R
I	:	Second moment of inertia, kilograms-metre^2
I_θ	:	Torsional moment of inertia per unit length, kilograms-metre
K_θ	:	Equivalent flap spring stiffness, metre-Newtons/radians
K	:	Control system torsional stiffness, metre-Newtons/radians
m	:	mass per unit length, kilograms/metre
P	:	First moment of inertia, Kilograms-metre
q	:	Pitching angular velocity, radians/second
R	:	Radius of the rotor or length of the beam, metres
S	:	Torsional approximating functions
T	:	Centrifugal tension, Newtons
x	:	Nondimensional radial coordinate
β	:	Flapping angle, radians
θ_O	:	Collective pitch angle, radians
θ_T	:	Local twist angle, radians; = x θ_{Tt}
θ_e	:	Elastic angle due to the propeller moment, radians
v_i	:	Natural frequencies, nondimensionalized w.r.t.Ω
Ω	:	Rotor rotational speed, radians/second

*Presently Westland PLC, Helicopter Division

1 - Introduction

The current methods of assumed modes have not provided a consistent representation of a rotating nonuniform blade whose structural properties vary sharply or discontinuously along its length. For example, considering uncoupled flapwise motion and using the linear theory for deformation, the bending moment is equal to the discontinuous flexural rigidity multiplied by the second derivative of the deflection which has been assumed to be a series of continuous functions. Thus, the resultant moment is discontinuous. Meanwhile, these methods utilize the energy approach to construct the eigenvalue problem. This approach results in the disappearance of the derivatives of the flexural rigidity. Then, the problem of the bending moment discontinuity has been solved by either approximating the discontinuous structural properties by linear functions; Yntema (1955, ref. 1) or by modifying the eigenvalue problem by expanding the moment as a series in the second derivative of the deformation; Lang et al (1979, ref. 2). Both methods may be regarded as methods of averaging the effect of discontinuity and are not rigorous solutions to the problem.

The objective of this paper is to demonstrate that the Galerkin method in which the eigenvalue problem is constructed directly from the equation of motion is also applicable to the case of nonuniform blades. This is achieved by using the theory of generalized functions in the mathematical manipulation of Heavside distributions. The frequencies obtained from this method are the same as those obtained from the energy methods. Nevertheless, the problem of inconsistency still remains. However, the advantage of the "Galerkin" method is that the method can be easily extended to non-linear and non-conservative problems; Bramwell (1976, ref. 3). The objective is also to remove the inconsistency mentioned above by using a finite element-like representation of the assumed modes. Then, the definitions of the equivalent flapping hinge offset and inertia terms for hingeless blades are reassessed in an attempt to make the simple flapping equation more representative. Also an equivalent elastic twist is proposed in order to partially compensate for the absence of the torsional analysis in the simple rotor programs.

2 - Assumed Modes Methods for Uniform Blades

The programs "FMODE" and "GMODE" are developed to calculate the uncoupled flapwise and torsional mode shapes and their natural frequencies. Polynomials; "$G_i(x)$" which satisfy all the boundary conditions as well as extra node conditions are used as approximating functions, and are automatically generated by these programs. The mode shapes "$g_k(x)$" are then calculated from:

$$g_k(x) = \sum_{i=1}^{N} G_i(x)\, C_i^{(k)} \tag{1}$$

where: "$C_i(k)$" is the ith element of the kth eigenvector.
"N" is the required number of modes.

The eigenvectors "$C_i(k)$" are evaluated by solving the following eigenvalue problem:

$$\sum_{i=1}^{N} (v^2 A_{\ell i} - B_{\ell i})\, C_i = 0.0 \quad , \quad \ell = 1,2,\ldots,N \tag{2}$$

where: "v" is the eigenvalue (the natural freqeuncy);
"$A_{\ell i}$" is an element of the inertia matrix
"$B_{\ell i}$" is an element of the stiffness matrix

"FMODE" uses Lagrange's method which constructs the eigenvalue problem from the energy consideration; hence for uncoupled flapwise motion:

$$A_{\ell i} = \int_0^1 m\, G_\ell\, G_i\, dx \tag{3}$$

$$B_{\ell i} = \int_0^1 [EI\, G_\ell^{''}\, G_i^{''}/(\Omega^2 R^4) + T\, G_\ell^{'}\, G_i^{'}/(\Omega^2 R^2)].dx \tag{4}$$

where: "m" is the mass per unit length
"x" is nondimensional radial coordinate
"EI" is the flexural rigidity
"T" is the centrifugal tension; $= \Omega^2 R^2 \int \text{mp dp}$
"Ω" is the rotational speed
"R" is the radius of the blade or the length of the beam
"'" indicates differentiation w.r.t.x

Meanwhile, "GMODE" uses the Galerkin method which forms the eigenvalue problem directly from the equation of motion. In this case "$B_{\ell i}$" becomes:

$$B_{\ell i} = \int_0^1 G_\ell [(EIG_i')'/(\Omega^2 R^4) - (TG_i')'/(\Omega^2 R^2)] dx \tag{6}$$

For uncoupled torsional motion the Galerkin method gives:

$$A_{\ell i} = \int_0^1 I_\theta S_\ell S_i \, dx \tag{7}$$

$$B_{\ell i} = \int_0^1 S_\ell [(GJ S_i')'/(\Omega^2 R^2) - I_\theta S_i] dx \tag{8}$$

where: "S_i" is the torsional approximating functions
"GJ" is the torsional rigidity
"I_θ" is the torsional inertia per unit length

Both programs lead to the same results when the structural properties are uniformly or continuously distributed along the blade.

It is worth mentioning that equation (4) can be also obtained by integrating equation (6) by parts if the approximating functions are of comparison type. The comparison functions satisfy the geometric and the natural boundary conditions.

Non-Rotating Uniform Beams

The accuracy of these programs is checked by comparing their results to the exact results of non-rotating uniform beams tabulated by Blevins (1979, ref. 4); Figures 1 to 4. Ten modes are used to obtain the frequencies listed in these figures. These figures indicate that the accuracy of the programs is reasonable. The natural frequencies of the transverse vibration are proportional to the parameter $(EI/mR^4)^{0.5}$. Meanwhile, the mode shapes are independent of the structural properties; ref. 4. The mode shapes of the bending moment are obtained by multiplying the flexural rigidity "EI" by the second derivatives of the mode shapes of the deflection; Figure 2. The natural frequencies of the torsional vibration are proportional to the parameter $(GJ/I_\theta R^2)^{0.5}$. The torsional mode shapes are independent of the structural properties. This only applies for the torsional vibration of fixed-free, fixed-fixed and free-free cases.

Rotating Uniform Blades

The flapwise natural frequencies; "v_i" are functions of the parameter $EI/(m\Omega^2R^4)$. However, there is no exact representation of these functions. Figures 5 and 6 show the flapwise mode shapes of an articulated blade (e = 0.0), and the corresponding normalized bending moment mode shapes. The first mode shape is a straight line. Consequently, no bending moment arises from this mode. Generally, the mode shapes of a rotating blade are functions of the structural properties and the rotational speed. The normalized bending moment mode shapes presented in Figures 6, 8 and 10 are calculated for a value of "m" equals to 7 Kg/m. Figure 6 indicates that the maximum value of the bending moment of an articulated rotor in a steady flight occurs at a radial position range of 0.6R-0.75R. Figure 7 shows the flapwise mode shapes of an articulated blade with flapping hinge offset. The first flapwise mode shape is not exactly a straight line. However, the contribution of this mode to the bending moment is very small; Figure 8. Figure 9 shows the mode shapes of uniform hingeless balde. In this case, the bending moment reaches its maximum value at the blade root; Figure 10.

Generally, the contribution of each mode to the bending moment can be calculated by multiplying the corresponding bending moment mode shape by the associated degree of freedom. Figure 11 shows the torsional mode shapes of a typical rotor blade. The control system flexibility gives rise to an equivalent spring stiffness "K_θ". The natural frequencies in this case depend on the parameter "$GJ/(I_\theta \Omega^2 R^2)$" as well as the parameter "$GJ/K_\theta R$" which is imposed on the eigenvalue problem when the boundary conditions are satisfied. Generally, the torsional mode shapes are independent of the rotor speed; ref. 3. Moreover, the difference between the square of each natural frequency and the square of the rotational speed is always constant and is equal to the square of the corresponding natural frequency of a non-rotating blade. Thus, the exact solutions of non-rotating beams can be used to describe the uncoupled torsional motion. Figure 12 shows the mode shapes of the torsional moment which are obtained by multiplying the torsional rigidity "GJ" by the first derivative of the mode shapes of deflection.

3 - Assumed Modes Methods for Nonuniform Blades

The eigenvalue problem deduced from the energy considerations does not involve any differentiation of the flexural rigidity term. Meanwhile, using Galerkin's method implies differentiation of this term. This may be a disadvantage if the flexural rigidity undergoes sudden changes; ref. 3. To illustrate this, the nonuniform distribution presented in Figure 13 is considered and "$B_{\ell i}$" of equation (6) or (8) is evaluated by the "GMODE" program as follows:

$$B_{\ell i} = \int_0^1 dB_{\ell i} \tag{9}$$

$$\int_0^1 dB_{\ell i} = \int_0^{x_1-\varepsilon} dB_{\ell i} + \int_{x_1+\varepsilon}^{x_2-\varepsilon} dB_{\ell i} + \ldots + \int_{x_L+\varepsilon}^{1} dB_{\ell i} \quad , \varepsilon \to 0.0 \tag{10}$$

$\int$ means that the integration is performed along several divisions with the flexural rigidity continuous and differentiable over each division. Then, the "GMODE" program is used to calculate the flapwise mode shapes and frequencies of a nonuniform blade; Figure 14. Although the mass and stiffness are increased considerably at the root portion of the blade, the natural frequencies "ν_i" are slightly higher than those calculated for a uniform blade (Figures 9 and 14). Meanwhile, the results of "FMODE" program (Lagrange's method) are more reasonable; Figure 15.

The disadvantage of Galerkin's method is removed by using the theory of "generalized functions" (e.g. references 5,6 and 7) which gives the following:

$$\theta_{xn} = \begin{matrix} 1 & x \geq x_n \\ 0 & x < x_n \end{matrix} \tag{11}$$

$$\delta_{xn} = \frac{d\theta_{xn}}{dx} \quad and \quad \delta'_{xn} = \frac{d\delta_{xn}}{dx} \tag{12}$$

$$\int_c^d F(x)\,\delta_{xn}\,dx = F(x_n) \quad and \quad \int_c^d F(x)\,\delta'_{xn}\,dx = -\left(\frac{dF(x)}{dx}\right)_{x=x_n} \tag{13}$$

where: "θ_{xn}" is the Heaviside distribution
"δ_{xn}" is the Dirac Delta at the point x_n, $c < x_n < d$
"F(x)" is a differentiable function for $c < x < d$

Now, the discontinuous distributions of the structural properties can be written as functions of Heaviside distributions. For example, referring to Figure 13 the distribution of "EI" becomes:

$$EI = f_1(x) - \sum_{n=1}^{L} f_{n,n+1}(x) \tag{14}$$

where: "L" is the number of points at which there are jumps in "EI" or its derivative, and

$$f_{n,n+1}(x) = f_n(x) \; - f_{n+1}(x)$$

Substituting these distributions into equations (3), (8), (9) and (10), differentiating using equation (12) and integrating using equation (13) to obtain the following (see ref. 8 for details):

$$A_{\ell i} = \int_0^1 dA_{\ell i} \tag{15}$$

$$B_{\ell i} = \int_0^1 dB_{\ell i} + \sum_{n=1}^{L} (G_\ell' G_i'' f_{n,n+1} - G_\ell G_i'' f_{n,n+1}' - G_\ell G_i''' f_{n,n+1})_{x_n} / (\Omega^2 R^4) \tag{16}$$

$$B_{\ell i} = \int_0^1 dB_{\ell i} - \sum_{n=1}^{L} (S_\ell S_i' f_{n,n+1})_{x_n} / (\Omega^2 R^2) \tag{17}$$

$\int dA_{\ell i}$ is evaluated from either equation (2) or (9). $\int dB_{\ell i}$ of equations (16) and (17) are evaluated from equations (8) and (9).

The mode shapes and the natural frequencies obtained from the modified Galerkin method are very close to those obtained from Lagrange's method; Figure 15. However, Galerkin's method can be easily extended to non-linear and non-conservative problems. Meanwhile, both methods do not yet provide a consistent relation between the moment and the deflection. As a result of this, the calculated mode shapes of the bending moment are discontinuous functions; Figure 16.

The solution of this problem is achieved by implementing a finite element-like technique for the assumed modes. To illustrate this, consider that the discontinuity of the stiffness occurs at one point on the blade, and consider the flapwise motion. In this case, the blade is divided into two divisions, the stiffness of each division is continuous. The approximating function of each mode is represented by two polynomials. The first polynomial satisfies the boundary conditions at the blade root and the compatibility conditions at the point of discontinuity. The second polynomial satisfies the boundary conditions at the blade tip and the compatibility conditions at the point of discontinuity. The compatibility conditions are as follows:

- The deflection and the slope obtained from the first polynomial at the point of discontinuity are equal to those obtained from the second one at the same point.
- The bending moment and shear force calculated at the point of discontinuity from the stiffness and the polynomial derivatives of the first division are equal to those calculated from the stiffness and the polynomial derivatives of the second division.

The above described approximating functions are then substituted into the equations presented in section 2 and the integrations are evaluated as demonstrated by equation 9. The flapwise mode shapes and the natural frequencies obtained by using this method are shown in Figure 17. The consistent continuous trend of the bending moment and the shear force are shown in Figures 18 and 19. The mode shapes of the shear force; "F_i" are calculated as follows:

$$F_i(r) = [EI g_i''(r)]' - T g_i'(r) \tag{18}$$

Figures 20 and 21 show a comparison between the results of this method and those of Lang et al (1979, ref. 2).

4 - Simplified Blade Flexibility Analysis

Generally, the contribution of the fundamental modes of motion to the rotor behaviour is more than that of the other modes. Therefore, utilizing the fundamental modes as the principal rotor design variables provides an acceptable engineering accuracy. In this section, the first modes of the flapwise and torsional motions are considered.

Flapping motion

Young (1962, ref. 9) introduced the concept of the flapping hinge offset for hingeless blades. Young's theory has been adopted ever since. The flexible blade has been replaced by a virtual rigid blade with a virtual flapping hinge and spring. The straight line representation of the first mode has been utilized then to calculate the flapping hinge offset from Southwell's formula (1921, ref. 10). This formula relates the flapping frequencies of a rotating blade to those of a non-rotating one. Following from Young's analysis, the first and second moment of inertia which appear in the flapping equation are those of a rigid blade about the virtual flapping hinge. Meanwhile, the virtual spring stiffness is equal to the square of the fundamental frequency of the non-rotating blade multiplied by the second moment of inertia.

On the other hand, if the rotor hub is pitching with constant angular velocity "q", the mode response equation of the flapwise first mode becomes:

$$\beta'' + \Omega^2 v_1^2 \beta = [\int \frac{\partial F}{\partial r} g_1(r)\, dr - 2\Omega\, q\, sin\psi \int rmg_1(r)\, dr]/\int mg_1^2(r)\, dr \qquad (19)$$

where: "β" is the flapping angle
"∂F/∂r" is the aerodynamic load per unit span
"r" is the radial coordinate

The flapping equation of the virtual rigid blade is:

$$\beta'' + \Omega^2 \lambda_{\beta k}^2 \beta = [\int \frac{\partial F}{\partial r} (r - eR)\, dr - 2\Omega\, q\, sin\psi\, \lambda_\beta^2 I]/I \qquad (20)$$

where:

$$\lambda_\beta^2 = 1 + ePR/I \quad and \quad \lambda_{\beta k}^2 = \lambda_\beta^2 + K/\Omega^2 I$$

"K" is the equivalent spring stiffness
"e" is the equivalent hinge offset
"P & I" are the first and the second moment of inertia

Equation (19) may be regarded as an exact representation of the flapping motion. Meanwhile, equation (20) provides an approximate representation of this motion. Thus, it may be argued that the best definitions of the equivalent flapping hinge offset, inertia terms and spring stiffness are the definitions which bring the flapping equation of the virtual rigid blade as close as possible to equation (19). Therefore, the following definitions are obtained by direct comparison between the two equations.

$$I = \int m g_1^2(r)\, dr \qquad (21)$$

$$\lambda_{\beta k}^2 = \lambda_\beta^2 + K/\Omega^2 I = v_1^2 \qquad (22)$$

$$\lambda_\beta^2 = \int m r g_1(r)\, dr/I \qquad (23)$$

$$\int \frac{\partial F}{\partial r} g_1(r)\, dr = \int \frac{\partial F}{\partial r} (r - eR)\, dr \qquad (24)$$

Figures 22 to 27 demonstrate the differences between Young's definitions and the new definitions. The variation of the flapping frequency "v_1^2" of a uniform blade with the parameter "$EI/m\Omega^2R^4$" is shown in Figure 22. Then, the flapping hinge offset is calculated from equation (24) by assuming that "∂F/∂r" is proportional to "r^2" and compared to the value obtained from Young's definition; Figure 23. Young's approach results in high values of this offset. Consequently, the aerodynamic moment

about the virtual hinge will not represent that moment which appears in equation (19). Furthermore, the local velocity due to the flapping will be in error especially near the tip of the blade. The significance of the frequency "$\lambda_\beta{}^2$"; Figure 25 is associated with the pitch and roll of the rotor. Figure 26 shows a comparison between the values of the virtual spring stiffness. At this stage, it seems that the differences between the parameters of both approaches are considerable. However, the hub moment, and consequently the control power and angular rate of damping obtained from the new definitions are slightly higher than that of Young; Figure 27. The hub moment; "M_h" due to the first mode is calculated from the following equation:

$$M_h = \Omega^2 \beta \, (v_1^2 - 1) \int_0^1 m \, g_1(r) \, r \, dr \tag{25}$$

The Equivalent Twist

It is widely known that the rotor load programs underestimate the value of the collective pitch angle for a required thrust when the torsional analysis is not included (e.g. ref. 11). For a typical rotor, the difference between the actual collective pitch angle and the predicted one may reach a value of around two degrees. The introduction of an equivalent twist in order to compensate for this shortcoming is rather cumbersome. The elastic torsional deflection depends on the geometry of the blade section, the value of the control angles and the flight regime. Thus, an equivalent twist which may approximate this torsional deflection is expected to depend on many factors such as the positions of the aerodynamic centre, the feathering axis and the c.g. of the blade relative to the elastic axis. Nevertheless, an equivalent twist can be easily defined by considering the effect of the propeller moment only. The average value of the elastic angle is mainly influenced by this moment; since in a design which provides a minimum value of the control loads, the aerodynamic centre, shear centre and c.g. lie very close to or on the feathering axis.

Considering a rotor in hover, the elastic torsional deflection due to the propeller moment may be estimated as follows:

$$\left(\frac{GJ}{\Omega^2 R^2 I_\theta} \right) \frac{d\theta_e}{dx} = - \int_x^1 \theta \, dx \tag{26}$$

$$\theta = \theta_0 + \theta_T + \theta_e \tag{27}$$

where: "θ_0" is the collective pitch angle
"θ_T" is the local twist angle; = $x\theta_{Tt}$
"θ_e" is the elastic deflection due to the propeller moment

"θ_e" may be approximated to be

$$\theta_e = \theta_{eo} + \theta_{et} \sin(x\pi/2) \tag{28}$$

where: "θ_{eo}" is the elastic deflection at the root of the blade
"θ_{et}" is the elastic twist at the tip

Using the above equations and the boundary condition at the root gives the following equations:

$$\left(\frac{GJ}{\Omega^2 R^2 I_\theta} + \frac{4}{\pi^2} \right) \theta_{et} + \frac{\theta_{eo}}{2} = - \frac{\theta_o}{2} - \frac{\theta_{Tt}}{3} \tag{29}$$

$$\frac{2}{\pi} \theta_{et} + \left(\frac{K_\theta}{\Omega^2 R I_\theta} + 1 \right) \theta_{eo} = - \theta_o - \frac{\theta_{Tt}}{2} \tag{30}$$

The collective pitch angle that appears in these two equations can be replaced by the required thrust coefficient by using a simple formula. Then, the solution of the two equations will provide values for an equivalent pre- collective angle "θ_{eo}" and an equivalent twist angle "θ_{et}" which can be used in the

detailed analysis. For the typical rotor described in reference 8 the equivalent twist is found to be equal to -0.66 (wash-out). Meanwhile, the pre-collective pitch angle is found to be equal to -0.85 degrees. Therefore, the predicted collective pitch angle is expected to increase by approximately 1.4 degrees.

In forward speed equations (29) and (30) will provide an approximate value of "θ_{eo}" and "θ_{et}" due to the time independent part of the propeller moment. Nevertheless, these values are expected to partially improve the predictive capability of the simple rotor programs.

5 - Conclusions

It has been demonstrated that the "Galerkin" method is also applicable to the case of a blade whose structural properties vary sharply along its length. This was achieved by using the theory of the "generalized functions".

A finite element-like technique for the assumed modes was developed in order to obtain a consistent relation between the deflection of a nonuniform blade and its bending moment.

An equivalent flapping hinge offset and inertia terms were redefined in an attempt to make the simple flapping equation more representative. Also, an equivalent twist was proposed in order to partially compensate for the absence of the torsional analysis in a simple rotor program.

References

(1)	R.T. Yntema	Simplified Procedures and Charts for the Rapid Estimation of Bending Frequencies of Rotating Beams, NACA TN 3459, 1955.
(2)	K.W. Lang S. Nemat-Nasser	An Approach for Estimating Vibration Characteristics of Nonuniform Rotor Blades, AIAA Journal, September 1979.
(3)	A.R.S. Bramwell	Helicopter Dynamics, Edward Arnold, 1976.
(4)	R.D. Blevins	Formulas for Natural Frequency and Mode Shape, Van Nostrand Reinhold, 1979.
(5)	W. Kecs P.P. Teodorescu	Applications of Theory of Distribution in Mechanics, ABACUS Press, Tunbridge Wells, Kent, England, 1974.
(6)	Lighthill	Fourier Analysis and Generalized Functions, Cambridge University Press, 1966.
(7)	F. Farassat	Discontinuities in Aerodynamics and Dynamics: The Concept and Application of Generalized Derivatives, Journal of Sound and Vibration 55(2), 165-193, 1977.
(8)	H. Azzam	Investigation of Single and Twin Rotor Behaviour, Dissertation Submitted for the degree of Ph.D., Southampton University, 1986.
(9)	M.I. Young	A Simplified Theory of Hingeless Rotors with Application to Tandem Helicopters, 18th Annual National Forum of the A.H.S., 1962.
(10)	R.V. Southwell B.S. Gough	On the Free Transverse Vibration of Air-Screw Blades, A.R.C., R&M 766, 1921.
(11)	W. Johnson	Helicopter Theory, Princeton University Press, 1980.

Acknowledgement

The support of Procurement Executive, Ministry of Defence is gratefully acknowledged.

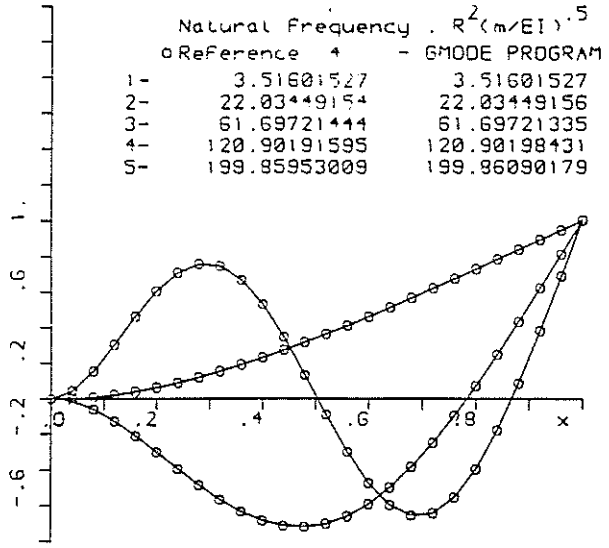

FIG.1 TRANSVERSE MODE SHAPES OF NON-ROTATING UNIFORM BEAM ,clamped-free

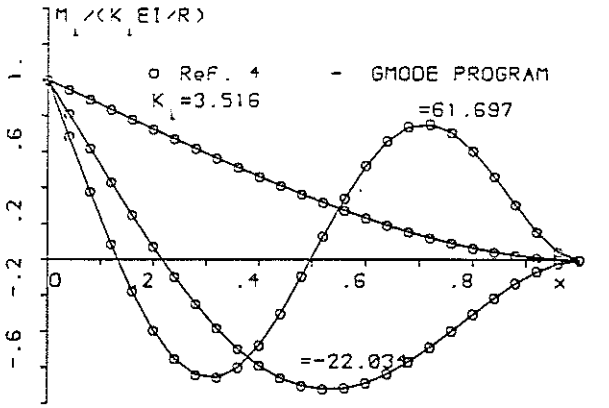

FIG.2 BENDING MOMENT MODE SHAPES OF NON-ROTATING UNIFORM BEAM ;clamped-free

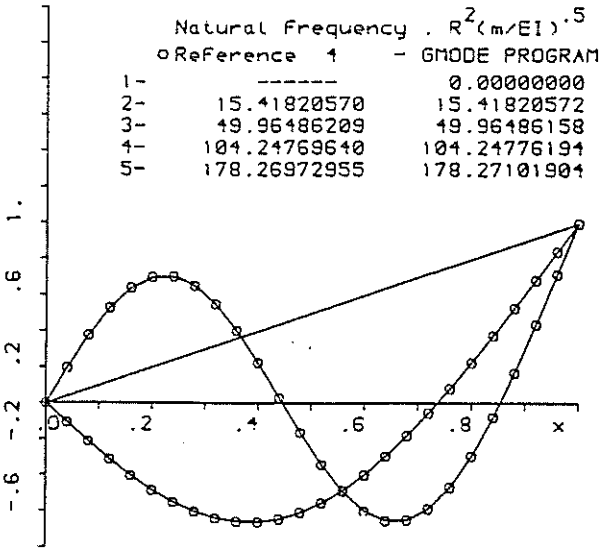

FIG.3 TRANSVERSE MODE SHAPES OF NON-ROTATING UNIFORM BEAM ;pinned-free

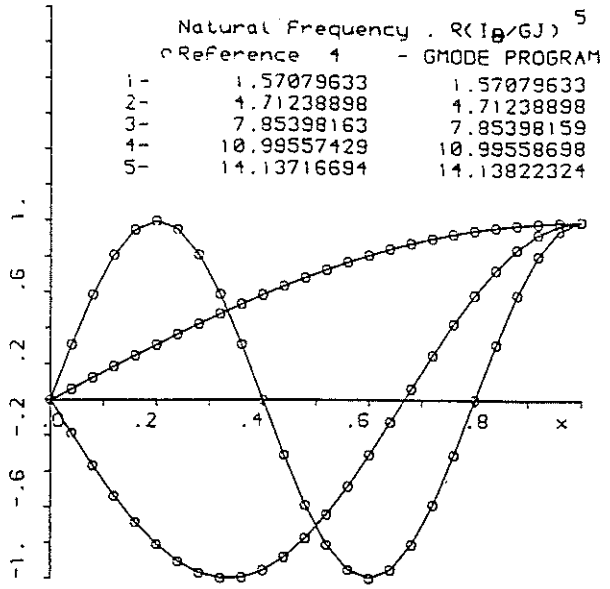

FIG.4 TORSIONAL MODE SHAPES OF NON-ROTATING UNIFORM CIRCULAR BEAM ;clamped-free

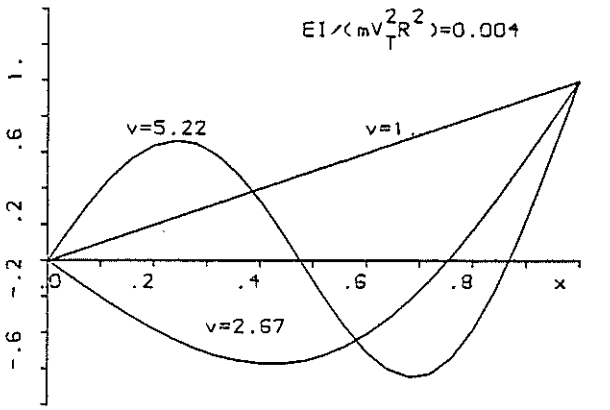

FIG.5 FLAPWISE MODE SHAPES OF UNIFORM ARTICULATED ROTOR BLADE ; e=0.0

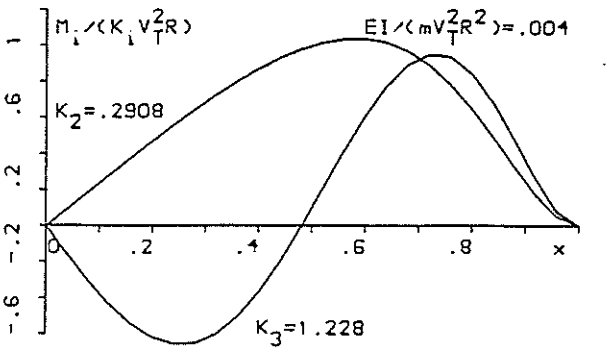

FIG.6 BENDING MOMENT MODE SHAPES OF UNIFORM ARTICULATED ROTOR BLADE ;e=0.

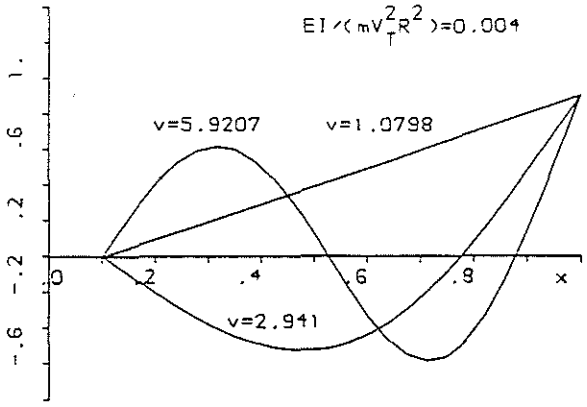

FIG.7 FLAPWISE MODE SHAPES OF UNIFORM ARTICULATED ROTOR BLADE ;e=0.1

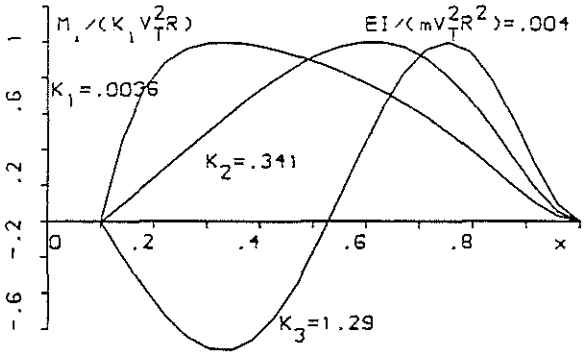

FIG.8 BENDING MOMENT MODE SHAPES OF UNIFORM ARTICULATED ROTOR BLADE ;e=0.1

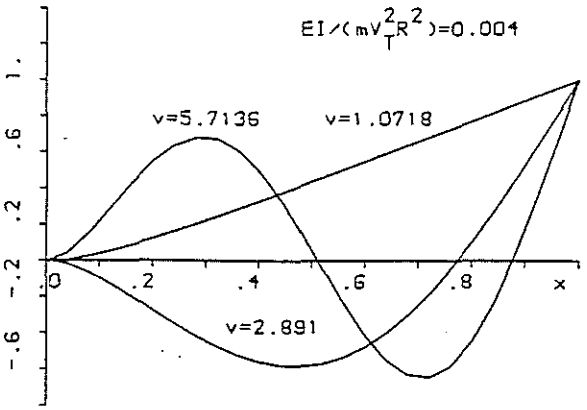

FIG.9 FLAPWISE MODE SHAPES OF UNIFORM HINGELESS ROTOR BLADE ;e=0.0

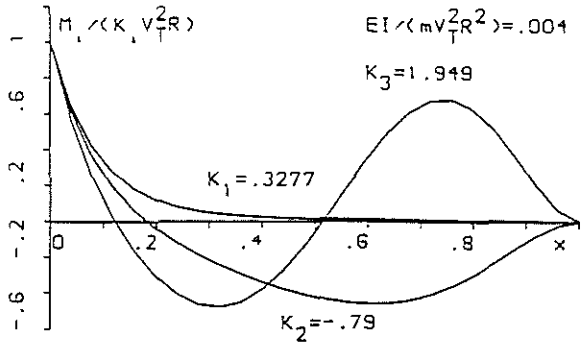

FIG.10 BENDING MOMENT MODE SHAPES OF UNIFORM HINGELESS ROTOR BLADE

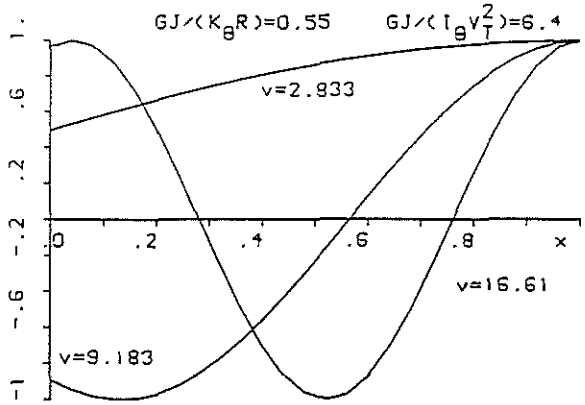

FIG.11 TORSIONAL MODE SHAPES OF A UNIFORM ROTOR BLADE

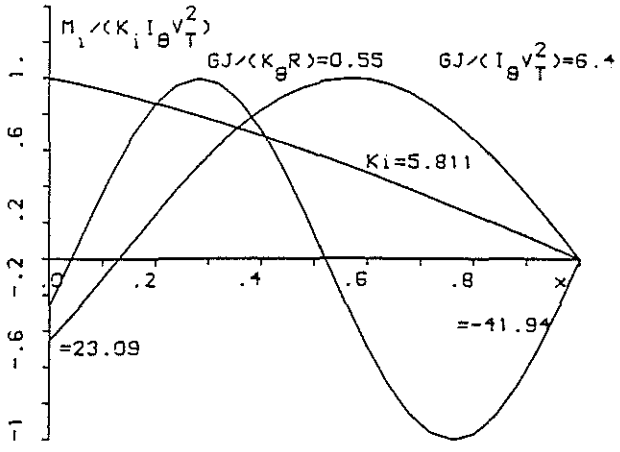

FIG.12 TORSIONAL MOMENT MODE SHAPES OF UNIFORM ROTOR BLADE

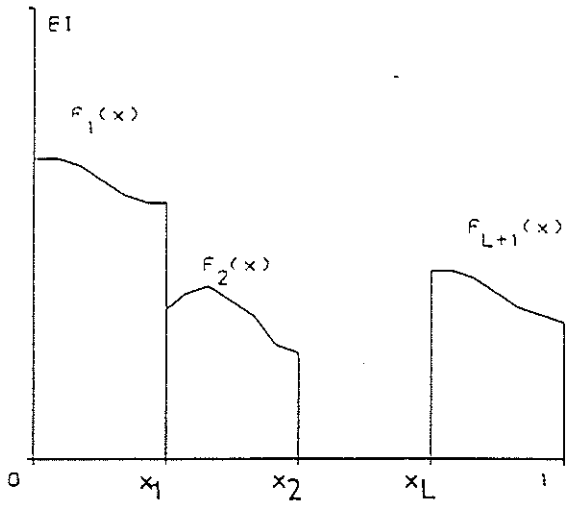

FIG.13 NONUNIFORM DISTRIBUTION OF EI

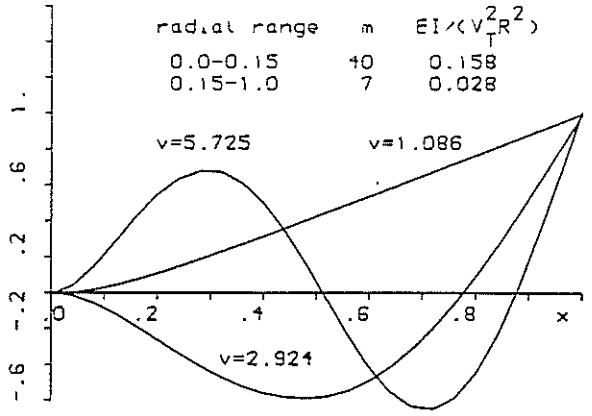

FIG.14 FLAPWISE MODE SHAPES OF NONUNIFORM ROTOR BLADE ;Galerkin's method

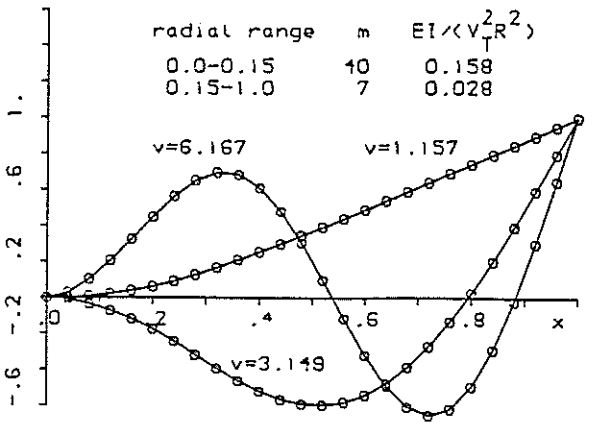

FIG.15 FLAPWISE MODE SHAPES OF NONUNIFORM ROTOR BLADE
o modified Galerkin's method
- Lagrange's method

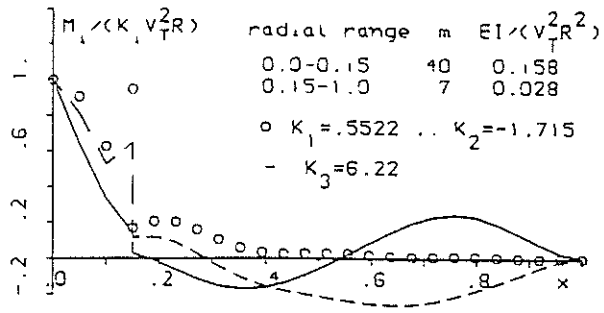

FIG.16 BENDING MOMENT MODE SHAPES OF NONUNIFORM ROTOR BLADE,Lagrange's method

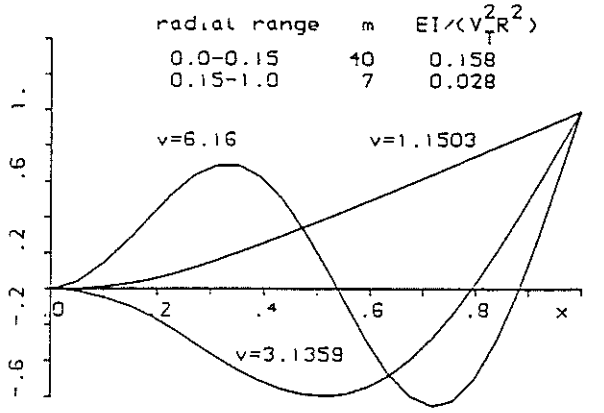

FIG.17 FLAPWISE MODE SHAPES OF NONUNIFORM ROTOR BLADE

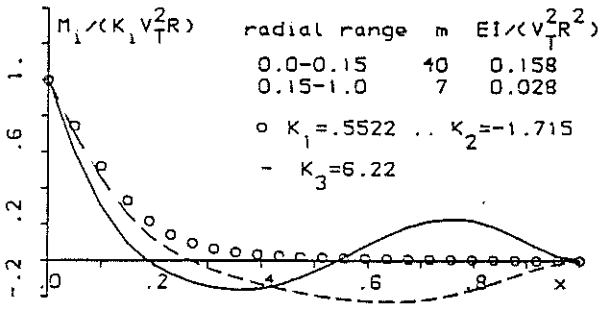

FIG.18 BENDING MOMENT MODE SHAPES OF NONUNIFORM ROTOR BLADE

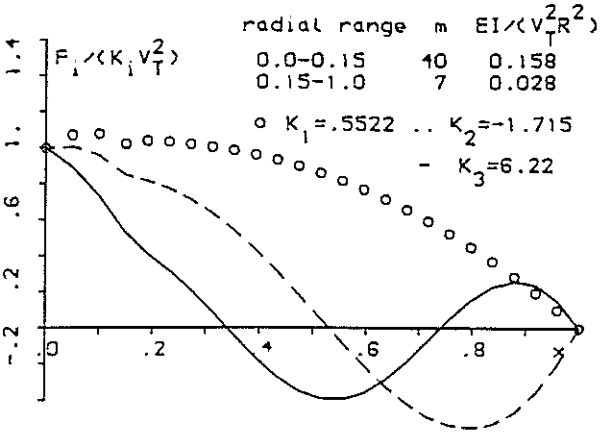

FIG.19 SHEAR FORCE MODE SHAPES OF NONUNIFORM ROTOR BLADE

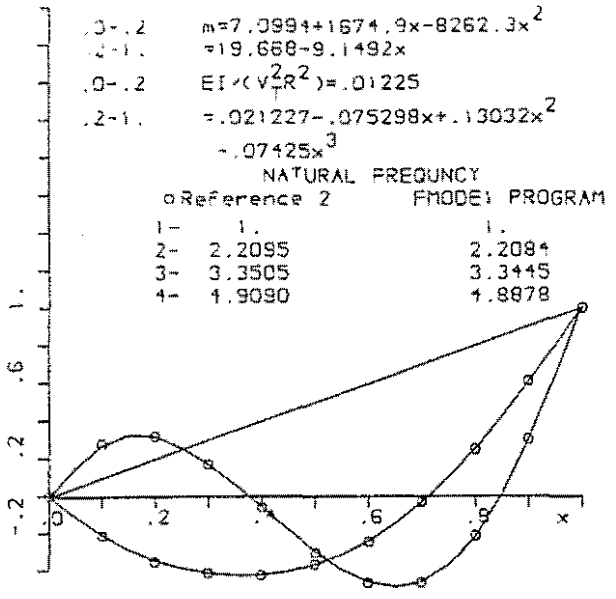

FIG.20 FLAPWISE MODE SHAPES OF NONUNIFORM ARTICULATED ROTOR BLADE ;e=0.

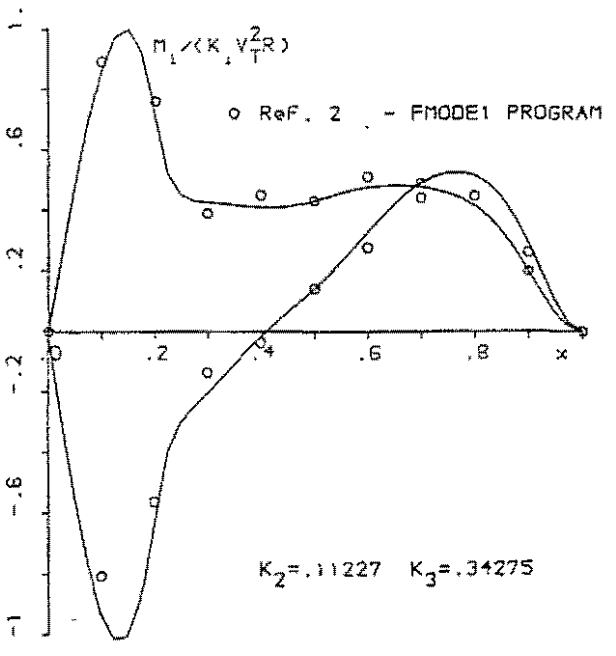

FIG.21 BENDING MOMENT MODE SHAPES OF NONUNIFORM ARTICULATED ROTOR BLADE

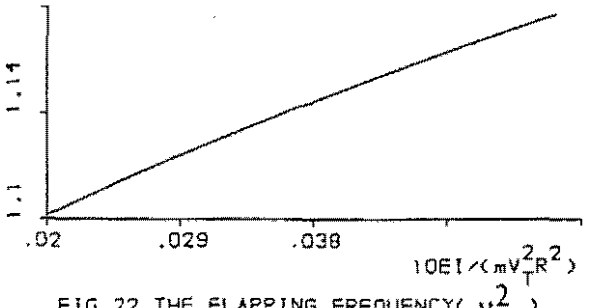

FIG.22 THE FLAPPING FREQUENCY(ν_1^2)

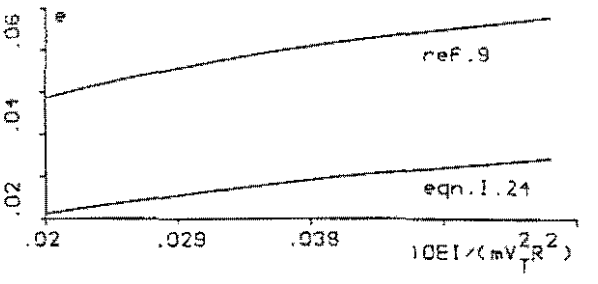

FIG.23 THE EQUIVALENT FLAPPING HINGE OFFSET

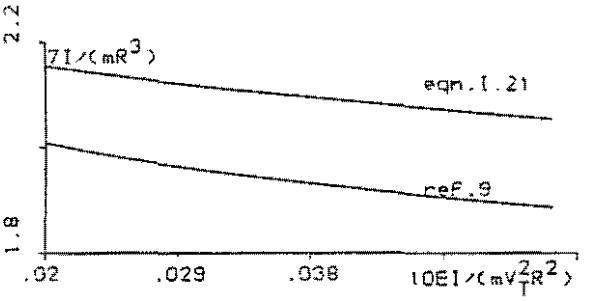

FIG.24 THE BLADE SECOND MOMENT OF INERTIA

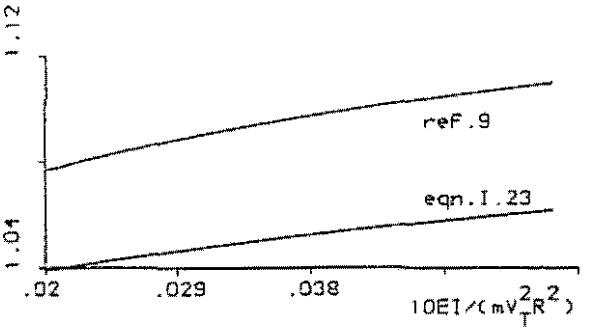

FIG.25 THE FLAPPING FREQUENCY(λ_β^2)

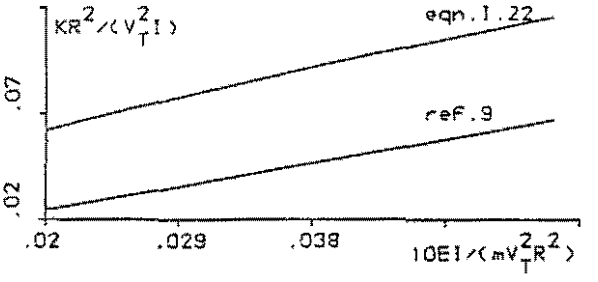

FIG.26 THE EQUIVALENT FLAP SPRING STIFFNESS

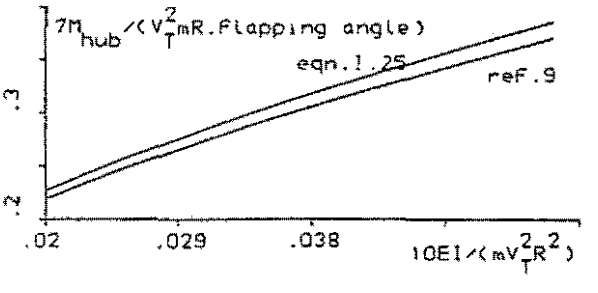

FIG.27 THE HUB MOMENT OF A HINGELESS BLADE